

MEASUREMENTS ON AIR BAR/WEB
INTERACTION FOR THE
DETERMINATION
OF STABILITY
OF A WEB

By

BRIGITTE BUSCH

Diplom-Ing. Degree in Mechanical and Aerospace Engineering

Technische Universitaet Muenchen

Munich, Germany


1993

Submitted to the Faculty of the
Graduate College of the
Oklahoma State University
in partial fulfillment of
the requirements for
the Degree of
MASTER OF SCIENCE
July, 1997


OKLAHOMA STATE UNIVERSITY

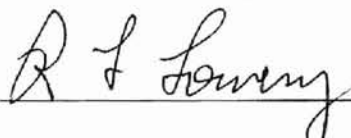
MEASUREMENTS ON AIR BAR/WEB
INTERACTION FOR THE
DETERMINATION
OF STABILITY
OF A WEB

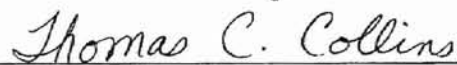
Thesis Approved:



Thesis Adviser







Dean of the Graduate College

ACKNOWLEDGEMENTS

I would like to thank Dr. Peter M. Moretti for serving as my adviser, for his invaluable assistance and support during my research work and throughout my entire graduate program. I also wish to express my appreciation to my Advisory Committee, Dr. Richard L. Lowery and especially Dr. C. Eric Price, for their helpful criticism and suggestions.

I would like to thank the Department of Mechanical and Aerospace Engineering, for providing me teaching and research assistantship during my graduate studies. I would like to express my sincere appreciation to Dr. Larry L. Hoberock, for offering me the opportunity of lecturing in the Department of Mechanical Engineering.

Special thanks to Ms. LeEtta Kitterman, Ms. Bonnie Milby and Ms. Janet Smith for their support and professional advice during my time of teaching as well as for my thesis work.

TABLE OF CONTENTS

1. INTRODUCTION	1
2. REVIEW OF EXPERIMENTS	3
3. OBJECTIVES	5
4. THE OPTICAL APPROACH	7
4.1. Digitizing the image	7
4.2. Capturing the image	9
4.3. The Digitized Photograph	12
5. DATA ANALYSIS	28
6. OBSERVATIONS	41
7. DISCUSSION	43
7.1. Influence of the Resolution	43
7.2. Vertical Distortion	43
7.3. Overlay Several Images	46
7.4. Curve Fit	47
8. CONCLUSIONS	52
9. FUTURE WORK	54

LIST OF FIGURES

FIGURE	PAGE
1.: AIRBAR SETUP IN A FLOTATION OVEN	2
2.: SCHEMATIC OF SETUP BY PINNAMARAJU	3
3.: PHOTOGRAPH OF THE EXPERIMENTAL SETUP IN THE LABORATORY	10
SCHEMATIC OF THE SETUP IN THE LABORATORY WITH ONE AIRBAR AND A PART OF THE WEB.	11
4.: PHOTOGRAPH OF THE WEB, AS IT WILL BE DIGITIZED BY THE FRAMEGRABBER BOARD	13
5.: DIGITIZED IMAGE AFTER APPLYING EDGE AND CONTRAST ENHANCEMENT OPERATIONS.	14
6.: SCHEMATIC THE ARRAY OF PIXELS AS IT IS STORED IN THE COMPUTER MEMORY.	15
7.: MATRIX REPRESENTATION OF THE IMAGE IN RAW-FORMAT.	17
8.: STANDARD EDGE DETECTION SOFTWARE APPLIED TO THE DIGITIZED IMAGE (FIG. 6)	18
9.: ONLY HORIZONTAL EDGES ARE DISPLAYED, AFTER SEVERAL FILTERS WERE 10.: APPLIED TO THE ORIGINAL DIGITIZED IMAGE (FIG. 6)	19
11.: SCHEMATIC, HOW TO FIND THE FIRST POINT ON THE CENTERLINE, WITH THE STARTING POINT BEING PICKED ANYWHERE IN THE NEIGHBORHOOD OF THE CENTER (HERE $N = 7$)	22
12.: DETECTED LINE, AS DISPLAYED ON THE SCREEN	25
13.: X-Y- GRID SYSTEM INTO WHICH THE PIXEL NOTATION IS TRANSFORMED. (THE ORIGIN BEING LOCATED AT THE LOWER LEFT HAND CORNER.)	26
14.: PIXEL LOCATIONS DISPLAYED AS THEY ARE STORED IN THE X-Y - COORDINATE SYSTEM	27
15.: FORCE BALANCE ON A CURVED INTERFACE IN 3 DIMENSIONS.	29
16.: TWO DIMENSIONAL CASE	30
17.: DISTORTION ANGLE (Θ) DUE TO THE ANGLE UNDER WHICH THE PHOTOGRAPH IS TAKEN.	34
18.: FIRST DERIVATIVE, APPROXIMATED BY CENTRAL DIFFERENCES FOR THE 19.: LOCATION Y OVER X.	39

20.: SECOND DERIVATIVE AS APPROXIMATED BY THE CENTRAL DIFFERENCES, FOR THE LOCATION Y OVER X.	40
21.: POLYNOMIAL FUNCTION AS DETECTED AND STORED IN THE PC.	45
22.: SECOND DERIVATIVE AS APPROXIMATED BY THE CENTRAL DIFFERENCES, FOR THE LOCATION Y OVER X. (AGAIN THE BLUE SHOWS THE 3-POINT FORMULA, AND THE PINK THE 5-POINT FORMULA.)	46
23.: SIMULATED CURVE AS IT IS DIGITIZED BY THE FRAME GRABBER (BLUE) AND ITS CURVE FIT (SIN-FUNCTION = PINK, POLYNOMIAL = YELLOW).	48
24.: SECOND DERIVATIVE USING CURVE DETECTED FROM THE ORIGINAL PHOTOGRAPH AND THE CURVE FIT WITH A SIN-FUNCTION (PINK) AND A SECOND DEGREE POLYNOMIAL (YELLOW).	50
25.: SECOND DERIVATIVE APPLIED TO THE CURVE FIT OF THE ORIGINAL LABORATORY SETUP. (PINK = DERIVATIVE OF THE SIN-FUNCTION, YELLOW = DERIVATIVE OF THE POLYNOMIAL).	51

NOMENCLATURE

D	projected height of the web (side view)
D'	projected height of the web as seen under an angle θ
P	pressure acting on the web
R	radius of curvature

GREEK LETTERS

σ	tension in the web, normal forces in the web
----------	--

1. INTRODUCTION

A web is a thin continuous strip of material such as paper, plastic film, or fabric that can be wound in a roll. Before it reaches its final stage as newspaper, plastic wrap, etc. it may undergo processes such as printing, coating and drying. Therefore, strips of substantial length have to be handled. In web processing, this is accomplished through automated equipment. This raises the possibility of web damage, especially in coating and drying processes. When drying the web in the flotation ovens or flotation dryers, the web is supported by impinging air jets.

The devices directing the air are called airbars, which come in many different shapes and sizes. Most important in this context, is that the air jets not only dry but also transport and guide the web. This is critical with these airbar-type supports, because there is no traction to control the cross machine motion of the long strips of material, as opposed to the use of rollers.

The setup of the airbars, alternating on the top and the bottom of the web, reduces the stiffness of the web in the lateral direction. Furthermore, for a small tilt angle of the web,

there can be substantial forces in the lateral direction. This can actually move the web so far in the cross machine direction that it might be damaged by hitting the sides of a flotation oven [Moretti], see Figure 1.

Having no contact between the supporting bar and the supported web makes the location of the web in the drying oven depend on the tension in the web and the pressure underneath it. Since the lift forces and tension need to be in equilibrium, the air gap between the support bar and web must be controlled closely. Otherwise, flutter and small vibrations of the web can damage the web or affect printing and/or coating process. These difficulties, when handling web material, make it necessary to be able to determine the position and the shape of the web throughout the coating and drying process.

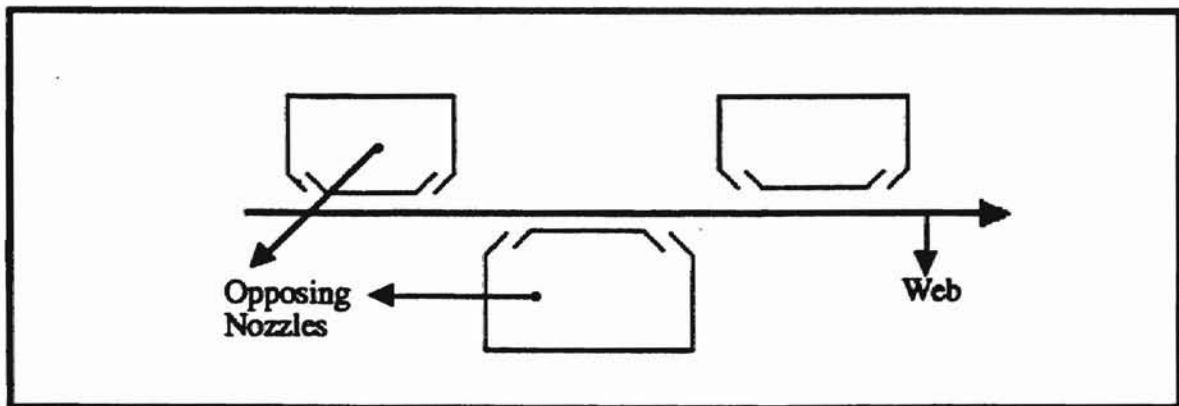


Figure 1: Airbar setup in a flotation oven

2. REVIEW OF EXPERIMENTS

Earlier experiments and measurements to determine the aerodynamic forces from an air support on a web were done by modeling the web as a rigid plate. In particular, Pinnamaraju (1992) compared several air support configurations for their influence on the pressure distribution along the web and the total lift forces,

Figure 2.

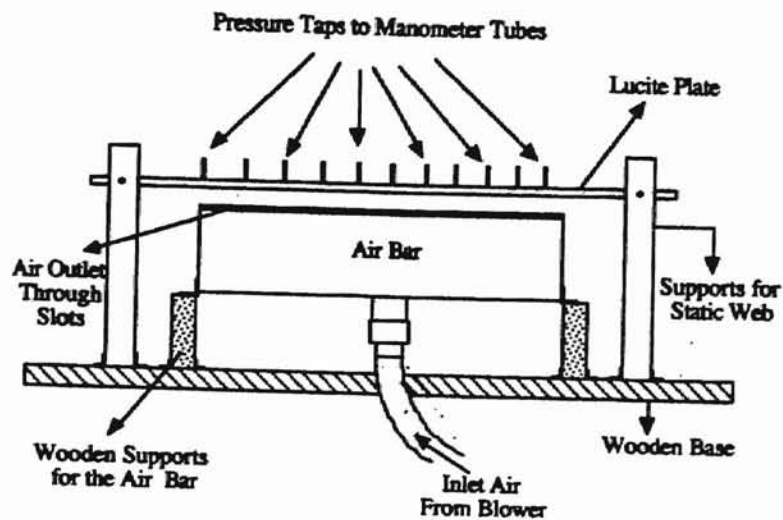


Figure 2: schematic of setup by Pinnamaraju

The lift forces are greatly influenced by the shape of the airbar and the flotation height of the web. Most airbars exert a positive aerodynamic lift on the web over an extensive range of gaps between the air support and the web. Air foil type bars behaved differently. Only for small flotation heights were the lift forces measured to be positive. At gap distances of 0.1 in., the lift force approached zero. But for all types of airbars the forces exerted on the web fell with increasing gap or flotation height. Less aerodynamic force signifies less control over the position of the web. Thus, the gap should be kept small. However, not too small, so that small disturbances will not result in contact between the airbar and the web. The critical point is that the forces are not known exactly. Unlike for a rigid plate, the real web is elastic and will not stay straight across the airbar. The tension in the web can be measured, but the flotation height depends on the tension as well as on the pressure created underneath the web. The gap can only be predicted knowing this pressure.

For a rigid static plate, pressure taps were inserted, by Pinnamaraju, along the plate and connected to a manometer. To reiterate, in the web handling process, the transported material is a thin web that is more or less flexible depending on the material, which is moving and not straight. Thus, it is not possible to insert pressure taps for measurements. Therefore, optical methods must be explored to enable prediction and analysis of the behavior of the web across the airbars.

3. OBJECTIVES

The objective of this project is to use optical methods to determine the shape of the web. Together with the knowledge about the tension applied to the material, the pressure and aerodynamic forces can be calculated from the shape of the web across the airbar, in particular the curvature (chapter 6).

As mentioned earlier, direct pressure measurements on a moving and more or less flexible web are not possible. Non-contact techniques need to be applied. The method used is an optical method, where the shape of the web is analyzed by using image analysis, and obtaining the necessary data from a photograph or video image, which is displayed in the computer.

The principle idea is to show whether an image, digitized and displayed in the computer can be used for further analysis of applied forces and pressures on the web. It was to be proven that standard devices like a video camera, a framegrabber and a 486-IBM compatible PC are sufficient to accomplish the basic steps. Those are

- Recording the web in the experimental setup
- Capturing the image

- Storing the image in the PC in a format that can be the basis for further data analysis
- Extracting the information about the shape of the web from the picture stored.

Since this is only a proof-of-principle, a time limitation on the image data analysis did not seem to be important. Which means, that the modeling of the dynamic behavior of the web was not a goal to be achieved.

Also, the number of interfaces, that were necessary because the experimental setup and the computer were in different locations, did not need to be taken into consideration.

4. THE OPTICAL APPROACH

4.1. Digitizing the image

The optical approach necessitates a means to capture images of the curved web and to analyze them. Generally, to analyze images the image/photo needs to be digitized. Any image processing software can then be applied to filter particular information from the picture or photograph.

To digitize an image, a video camera connected to a framegrabber board installed in a PC can be used. Another way would be to scan a photograph into the computer and create the digitized file of the image from the scanner. The approach chosen in the project was the former because a relatively inexpensive video camera and framegrabber board, can produce an adequate image much more conveniently and quickly.

The framegrabber used is a board that is widely available in computer stores and can be used with IBM or IBM compatible PC's. The model is VBFS 200, Creative Labs Inc. This framegrabber can only capture single images. More expensive and specialized boards can grab sequences of pictures at a rate of 30 images per second.

The framegrabber digitizes the pictures sent from a video camera output into the computer. Each picture is stored as a number of color coded “dots”. In the case of the VBFS 200, the number of “dots” or pixels is 372x496 for each picture. The first number stands for the number of “dots” per row and the second number for the number of “dots” per column.

When capturing the image, the choice is color or ‘black-and white’. For this project color is not needed and the second option was chosen. ‘Black-and white’ is not exactly black and white. In the display and storage of the image, this means that 256 different gray levels are coded and stored, where ‘0’ = black and ‘255’ = white. The number of 256 different possible gray levels explains itself from the way the pixels are stored in the computer. Each “dot” or pixel has 1 byte = 8 bit of memory. This can be pictured as 8 layers of information about the intensity of black or white. One bit can only read the value “1” or “0”, which translates to “on” or “off”. The 8 bits yield statistically $2^8 = 256$ possible combinations. Therefore, there are 256 possible levels of darkness, the so called gray levels.

Each pixel is coded with a number between “0” and “255”. This gives information about the darkness of the gray chosen to display this particular point in the picture. With the image being digitized at the resolution of 372x496, this means each picture needs a

storage of at least $372 \times 496 \times 256$ bits \sim 185kbytes. A 16-bit color image the same size would need a storage space of approximately 550Mbytes. This is one of the two main reasons why, in this project, only gray scale images were used. The other reason is that most of the image processing operations, and especially the edge detection operations, are a lot easier and faster for a 256-gray scale image than if they were applied to a 16-bit color image.

In this project, it is the shape of the web that is of interest. It can be ascertained by using edge detection applications and to determine the two edges of the web, and calculating an averaged slope and curvature between these two sides. Another possible way is to detect the center of the web by using a centerline, drawn on the web or (for more general purposes) projected on it, and directly detecting that line as the representative of the location of the web.

4.2. Capturing the image

For this project the web was initially photographed. The camera was setup in a way such that the picture would be taken from the side under an angle of 15° . (see Figure 3)

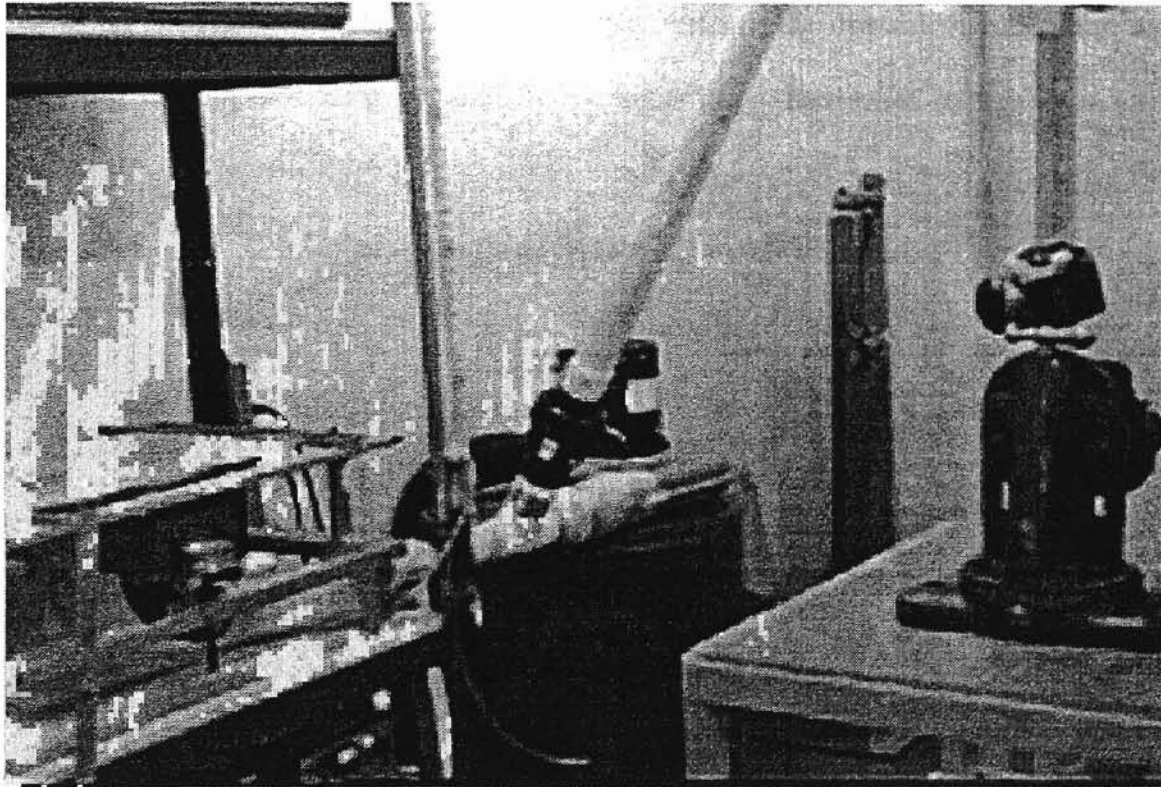


Figure 3: Photograph of the experimental setup in the laboratory

Because there are no substantial frictional forces, any motion in the cross machine direction would result from the forces in the upward direction, directly dependent on the tension and curvature of the web.

Therefore, the main plane of interest is the x - z plane. The z -direction is the direction of motion, that is determined by the pressure and the lift forces exerted on the web. Once these forces are known, the disturbances in the cross machine direction, or in the x - y

plane, are only dependent on the total resultant force in the upward direction and any occurring tilt angle of the web, as explained earlier in the Review of Experiments. (see Figure 4)

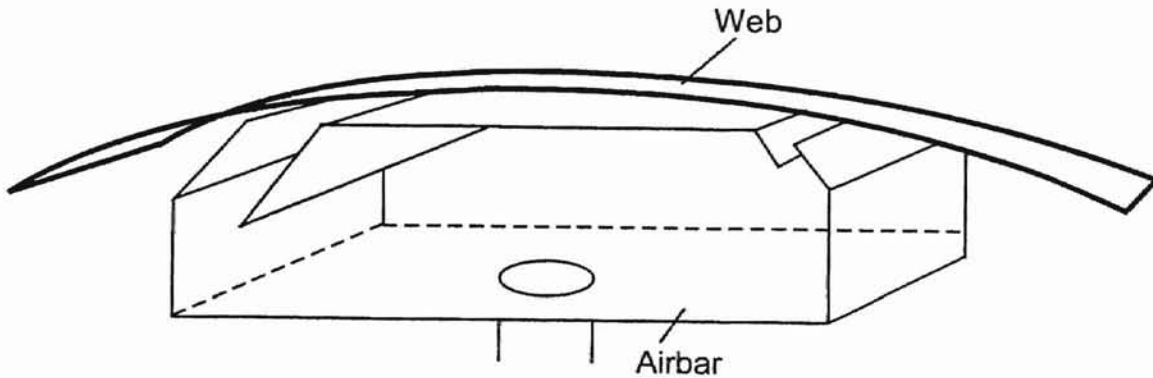


Figure 4: Schematic of the setup in the Laboratory with one airbar and a part of the web.

The video camera was not directly used for capturing the picture, and as input to the PC, because the experimental setup and the computer were in different locations, necessitating the photograph. Live display of the picture, and freezing it on the screen showed a high quality. Some of this quality was lost once the image was captured by the frame grabber. This arises because the live display basically bypasses the frame grabber, at least concerning the resolution. Live display means that the video camera feeds a signal

into the frame grabber which is unchanged and uncompressed sent to the screen. Therefore, the display quality of a live image depends only on the screen setup of the PC. As soon as the picture is stored, with the attributes that the frame grabber attaches to it, the resolution is fixed to 372x496 or vice-versa and, for this case, 256 gray levels.

4.3. The Digitized Photograph

The consequence was a visible drop in quality, especially the sharpness of the edges and details. (see Figure 5)

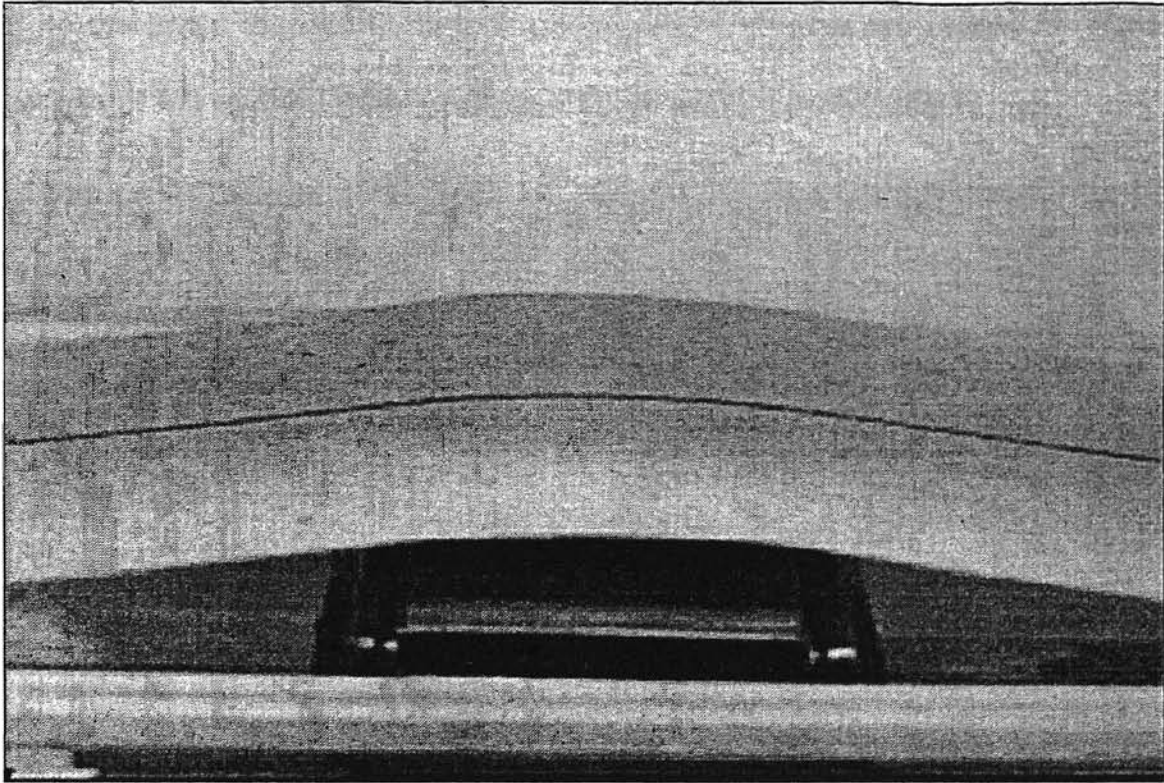


Figure 5: Photograph of the web, as it will be digitized by the framegrabber board

Several filter, edge enhancement and contrast enhancement operations were performed to the original image to give a picture with bigger contrast and enhanced edges.

All these operations are standard in any image processing package, available for the frame grabber or for a works station. The ones that were used here were Khoros and paintshop pro.

Once the image showed the pattern, that seemed to be most appropriate for further analysis, it was stored as the new version of the photograph. (see Figure 6)

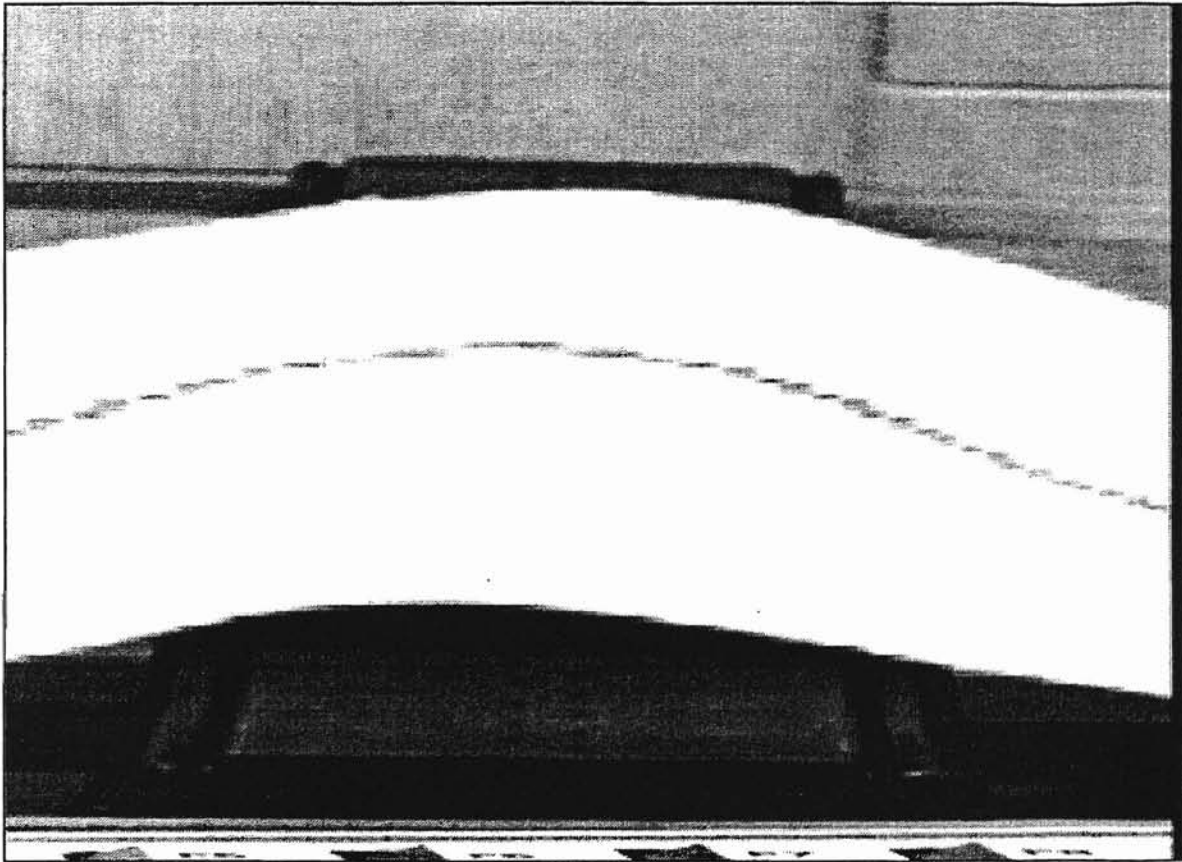


Figure 6: Digitized image after applying edge and contrast enhancement operations.

As described earlier, the images are stored in numbers that represent the gray scale intensity. Each pixel gets its intensity according to its location in the picture.

Once digitized, the picture can be interpreted as a matrix of 372x496 pixels. The way it is stored in the computer, though, is not exactly like a matrix. The actual image is an array

of numbers stored line by line, which starts at the upper left hand corner of the picture and ends in the lower right hand corner.(see Figure 7)

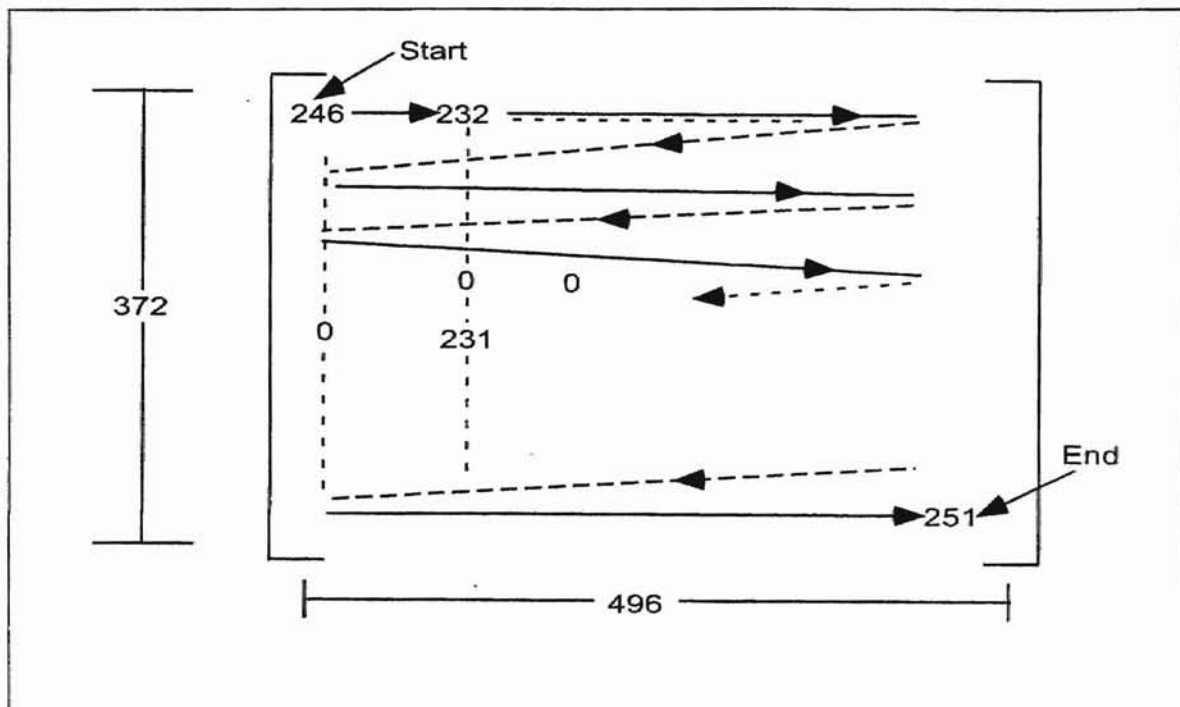


Figure 7: Schematic of the array of pixels as it is stored in the computer memory.

Another characteristic is that, once the frame grabber stores the image, it is in a pcx (pixel), bmp (bitmap) or tif (tiff) format. This means that, according to the format chosen, the file has a different compression format and therefore a different header up front.

It is not necessary to know all the different ways of compressing an image, the basic idea of compressing an image is to reduce its storage space. For example, one way is done is by coding each line and using multiples, if the same shade occurs more than once. The coding information is usually given in the header. Nevertheless, it is not simple to decode and decompress all these different formats by hand. Fortunately, this is not necessary.

Commercial software can convert any pixel-, bitmap-, tiff-, or other compression file into a RAW-format.

Consequently, all the file contains is the raw data for each pixel, as a binary number. No headers are added, no compression format or coding is used. Reading this array as binary numbers and converting them into real numbers, and displaying those numbers in matrix format, would give the pixel notation of the image. Instead of a picture the intensities of gray levels for each pixel are given (see Figure 8).

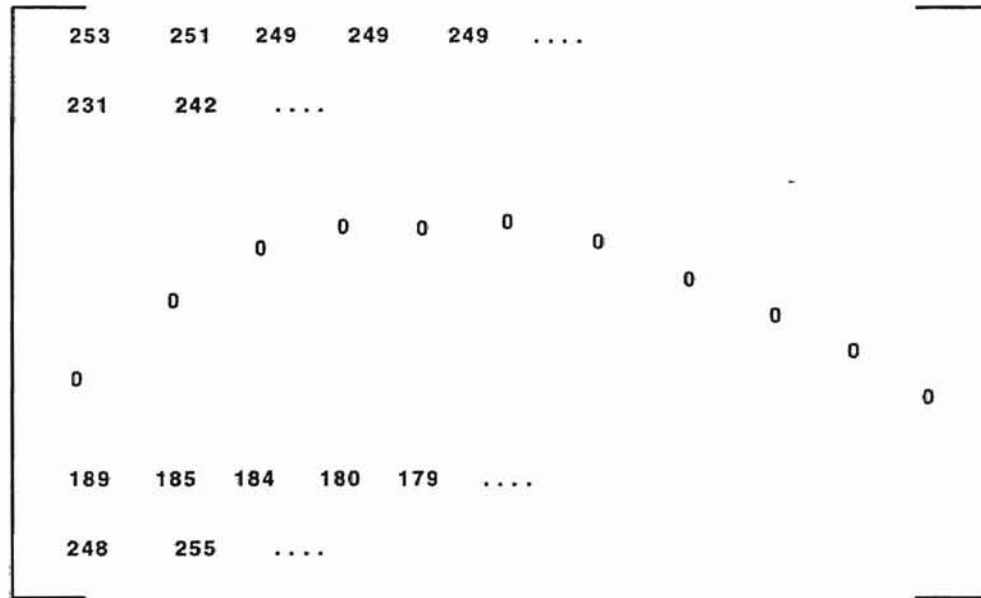


Figure 8: Matrix representation of the image in RAW-format.

The RAW-format is very helpful to detect edges or, for this project, to determine the location of the web.

As several different experiments showed, the standard edge detection packages, available with any image processing software, did not give the desired results. Since the image has more edges than just the two resulting from the web, any edge detection software will detect all these edges and display them. (see Figure 9)

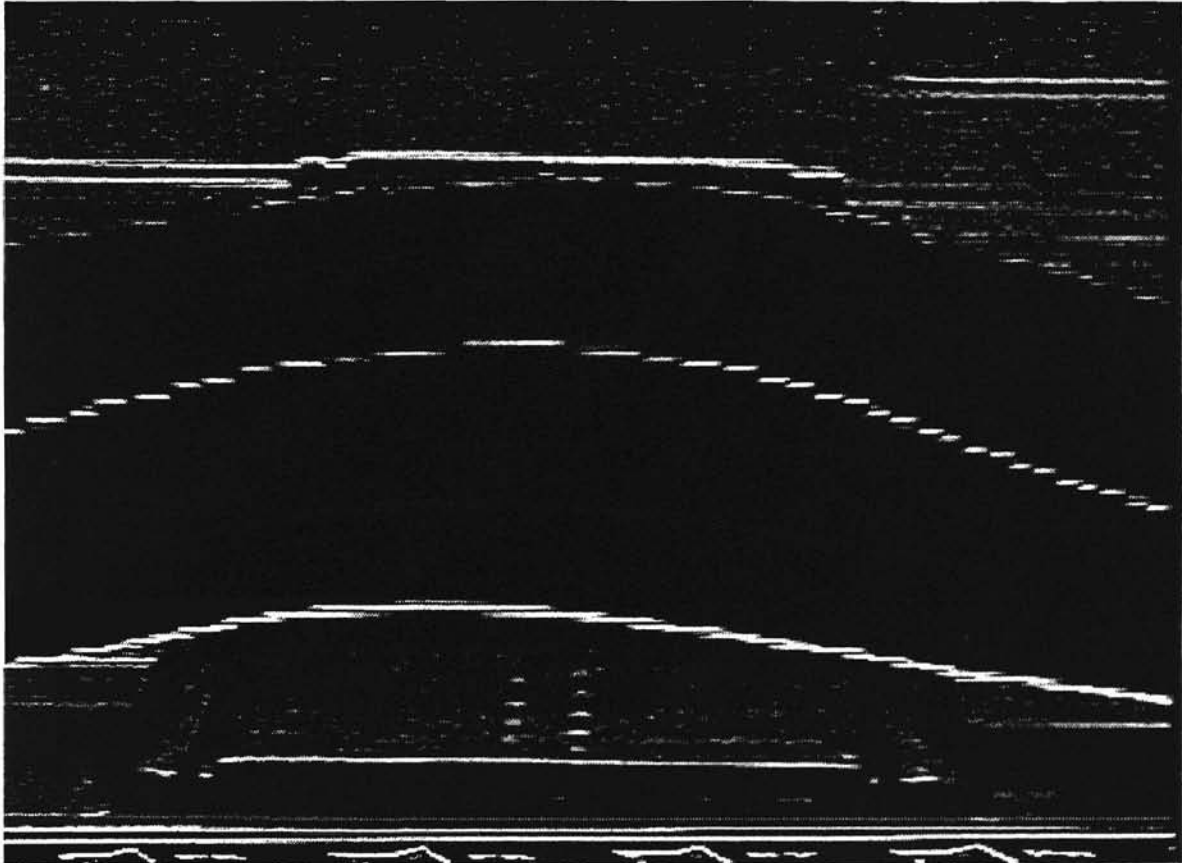


Figure 9: Standard edge detection software applied to the digitized image (Fig. 6)

Without a manual input or an applied filter, it is not possible to find only the web in the picture. Even after using different standard filter and only displaying the horizontal edges, too much background information was still being picked up (see Figure 10).

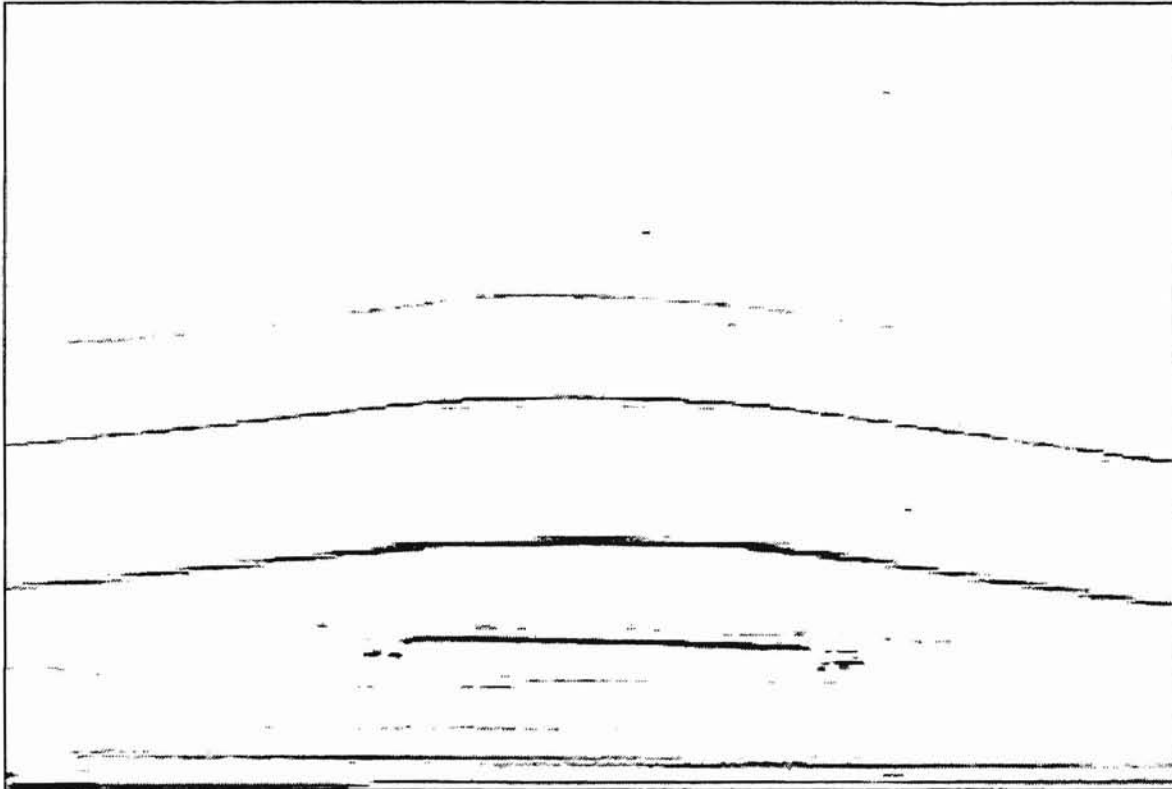


Figure 10: Only horizontal edges are displayed, after several filters were applied to the original digitized image (Fig. 6)

There are several options to solve this problem. One idea is to use the existing picture and apply several filters, if necessary geometric filters, to eliminate any unnecessary information. The problem arising with this solution is that, due to the change in location and especially shape, the filter would have to change constantly. This means that each single frame requires a new filter.

Another option is to change the experimental setup so that the photographs show only a distinct edge to the web. No background information will be picked up if, for example, the background is kept black and the web white. This would give the optimal contrast and best results, after being digitized and stored in the computer. The disadvantage of this is that it has very special requirements on the experimental setup, which means that a new series of photographs have to be taken. More importantly, it substantially limits the application of this method in a web line. Both of the foregoing solutions mentioned above have the great advantage that any standard edge detection software can be applied to gain the necessary information.

The third option looked at was a solution, not so much focusing on applying standard software as keeping the setup as general as possible, yet still gain the necessary information. This means that the photographs taken are being used, but the idea of applying standard filters, and standard edge detection software, was dropped. Instead, a software was developed that searches the digitized image, now stored in RAW-format, for the values that represent the web. For this purpose, a black line was drawn in the center of the web, which is representative of the web for further analysis. By determining the location of the black line, the location of the web is exactly defined and can be displayed as the vertical distance (z-direction) of points along the horizontal axis (x-direction). As mentioned earlier, this line could also be projected on the web. For simplification of the experiment, it was drawn with a marker on the white paper web.

The software, developed for detecting the centerline, starts at any given point, which should be in the vicinity of the centerline. It searches around that starting point for pixels that are part of the line drawn on the paper. This means that the software searches for pixel intensities “0” in the neighborhood of the starting point.

Once a pixel is located that is apparently a part of the centerline, then by checking the neighboring points to its right and left, the centerline will be traced throughout the whole image. The field, or window of searching, is variable. It can be changed by changing the input value for ‘N’ in the program code. A suitable number seems to be 15. If the original starting point for the search is close enough to the actual location of the center of the web, this number can be as low as 5.

The search for the black line within the window is referred to as “tracing the line”. Detecting the pixels that are elements of the centerline on the web becomes easier if it is taken into account that this line has to be continuous, with only small variations from one pixel to its neighbor. This is because the centerline, being part of the web, cannot contain any discontinuities or jumps. This allows the user, once the starting point is picked and the search around that point in the vertical direction identifies one pixel which is part of the centerline, to start tracing the center to the right and the left. (see Figure 11)

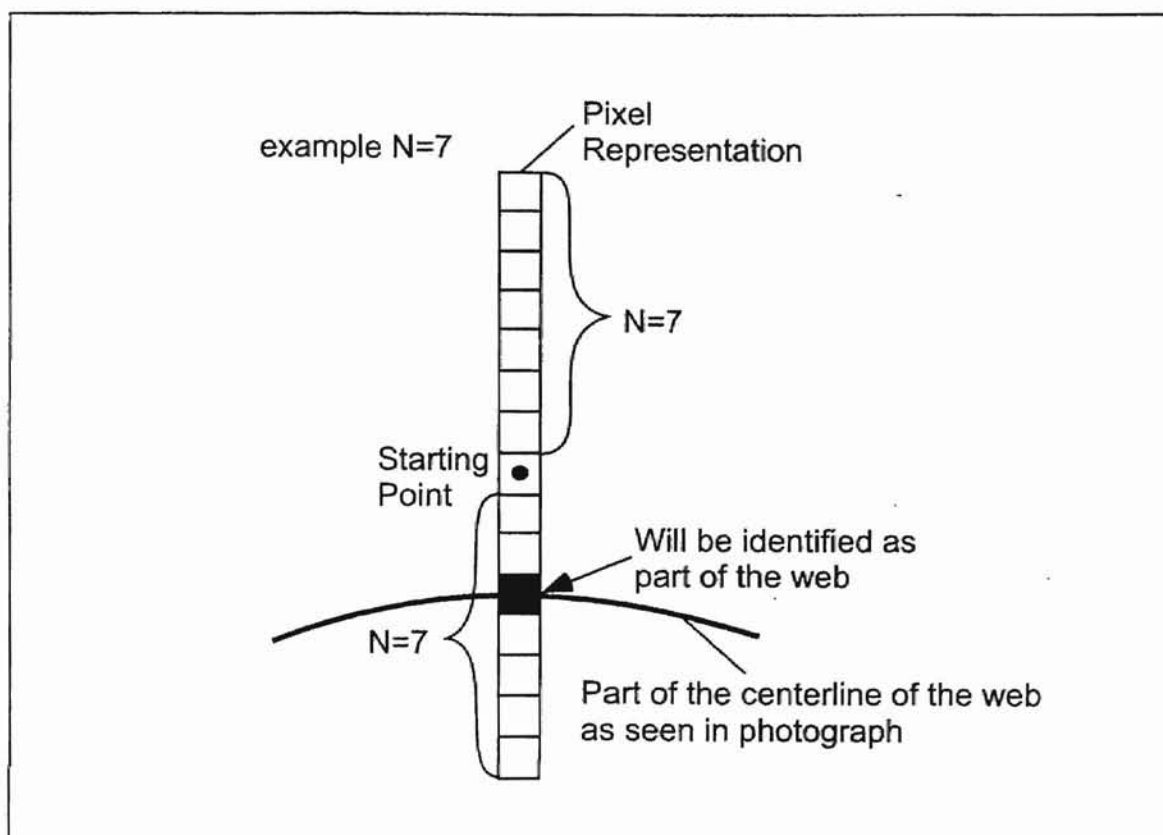


Figure 11: Schematic, how to find the first point on the centerline, with the starting point being picked anywhere in the neighborhood of the center (here $N = 7$)

“Tracing” means moving one pixel to the right and one pixel to the left and checking the RAW-data file for another black point closest to the previous one. Due to the fact that the web is continuous, it is known that the next element of the center should theoretically be in the same row or (at the most) one row above or below.

Because of some blurring effects while capturing the image and some error while digitizing the photograph, it can happen that the following pixel is 2 rows above or below the previous point. This was the maximum error observed, that needed to be taken into account.

This is not in agreement with the argument that the web is a continuous strip of material. Unfortunately, this type of error occurs when the photograph is digitized. The low resolution when capturing the image results in a blurring effect, that increases the width of the line and, at the same time, decreases the intensity stored for each pixel, from a black (represented by "0") to a dark gray (a value between 35 and 70). The original problem of detecting values that represent black in the image ("0's") has changed to detecting a value that is lower than a certain threshold value or a value, that is the lowest within the window looked at. This means that after identifying the first pixel that is a member of the black centerline, the neighboring points to its left and right need to be checked, whether they are a part of that same centerline or not. Each pixel will be compared to the pixel intensities in as many rows above and below as are defined by the value "N", staying in the same column. With this method, each pixel in the x-direction will be compared to N neighbors in its column (the z-direction), to make sure that, within the predefined window, the point with the lowest value for the color coding (=darkest pixel) will be determined. The value of N should not be less than 3, so it can be assured that the pixel identified is really a part of the centerline drawn on the web.

It is important that the value chosen for N is not too large. This could make the search run over the side of the web and again detect background edges. As mentioned earlier, the size of the window is very important for the outcome of the procedure and needs to be chosen very carefully. Hence, not larger than the size of the web itself as projected in the image, and no smaller than $N=3$. This guarantees the results expected, and it reduces significantly the time for the calculations. Only a small fraction of the RAW-data that originally represented the photograph needs to be analyzed. The disadvantage in this method is that the starting point needs to be picked within a reasonable close vicinity of the centerline of the web. It will be fairly difficult to pick this point automatically. The human judgment and eye is necessary to determine that, at least in the process used right now.

For a stationary web, the process could be automatic as long as the camera is mounted in such a way that the centerline falls within a vicinity of 35 to 50 pixels around the exact middle of the picture ($372/2$ and $496/2$). Then, the whole process could be started by assuming that the first point lies in the exact geometric center of the picture and ranging from there the search for the first point that is actually an element of the centerline. Several test runs showed that, as long as there are no optical obstructions, the line will always be detected correctly even with the starting point deliberately picked on one side of the web (50 pixels away from the actual center).

After the centerline has been detected, it is displayed on the screen, for reference.(see Figure 12)

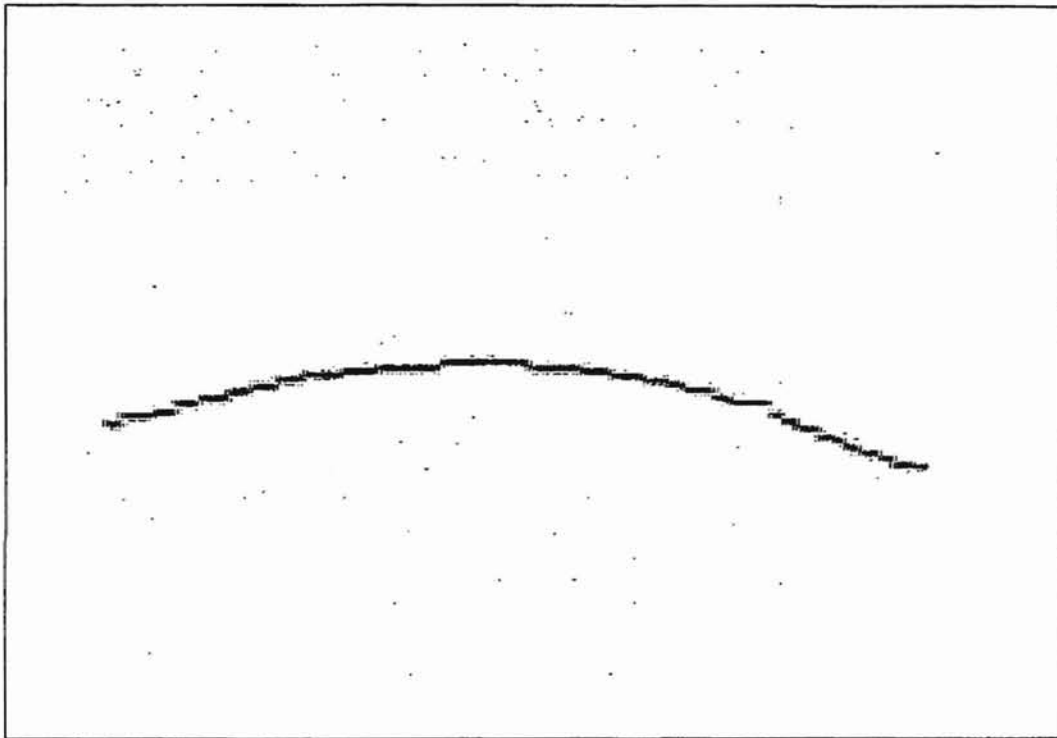
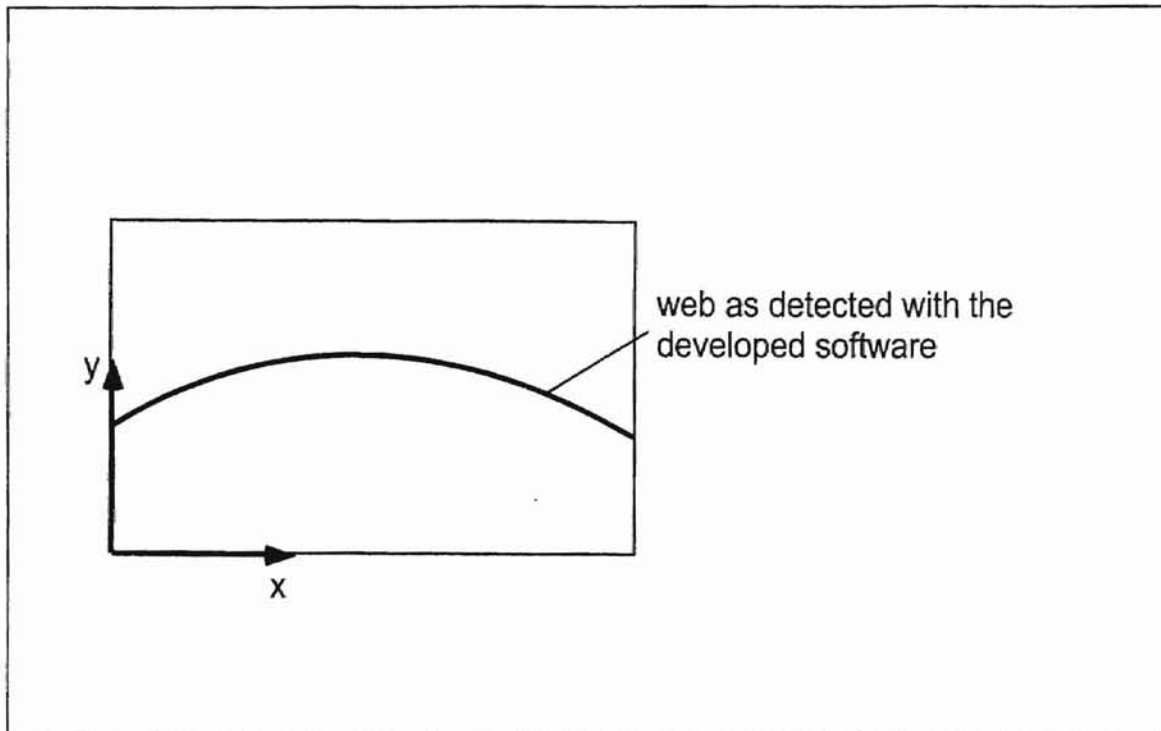


Figure 12: Detected line, as displayed on the screen

The points, that were determined to be part of the black line on the web, are stored in terms of a coordinate system. At first their location in the RAW-data file is stored in the memory and then with a coordinate transformation changed to a x-y-grid notation. The x-

coordinate is counting the pixels in horizontal direction, the y-coordinate those in the vertical direction. (see Figure 13)



**Figure 13: X-y- grid system into which the pixel notation is transformed.
(The origin being located at the lower left hand corner.)**

The origin of this coordinate system is placed into the lower left hand corner of the image, or the matrix notation representing the image. Again, displaying y over x gives exactly the same result as above. Therefore, this is a way of assuring that the coordinate transformation was done correctly. (see Figure 14)

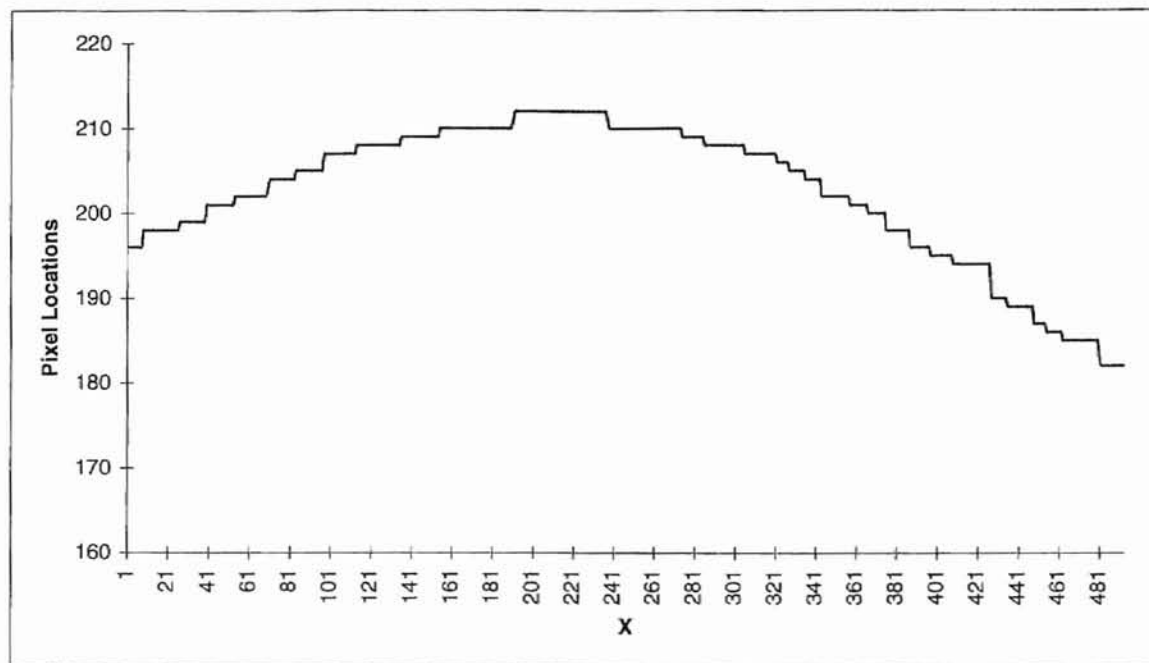


Figure 14: Pixel locations displayed as they are stored in the x-y - coordinate system

5. DATA ANALYSIS

As discussed in the earlier chapters, the goal of this project is to be able to determine the pressure distribution underneath the web by using optical methods and relating the shape of the web to the forces acting on the web.

The relationship between the pressure distribution underneath the web, the web tension, and the radius of curvature can be derived from the force balance across a curved interface. Taking a small section of a 3-dimensionally curved interface (see fig. 15) with the geometric dimensions being ds and dn , the pressure acting below the surface being P_I , and the pressure acting from above on the surface P_{II} , and normal force σ , the following relationships can be written.

Force Balance

$$(P_I - P_{II}) dnds = 2\sigma dn \left(\frac{\Delta\beta}{2} \right) + 2\sigma ds \left(\frac{\Delta\alpha}{2} \right)$$

$$(P_I - P_{II}) = \sigma \cdot \left(\frac{\Delta\beta}{ds} + \frac{\Delta\alpha}{dn} \right)$$

with:

$$dn = R_1 \Delta\alpha$$

$$ds = R_2 \Delta\beta$$

The Laplace - Young - Eq. Can be derived as:

$$(P_I - P_{II}) = \sigma \left(\frac{1}{R_1} + \frac{1}{R_2} \right)$$

Eq. 1

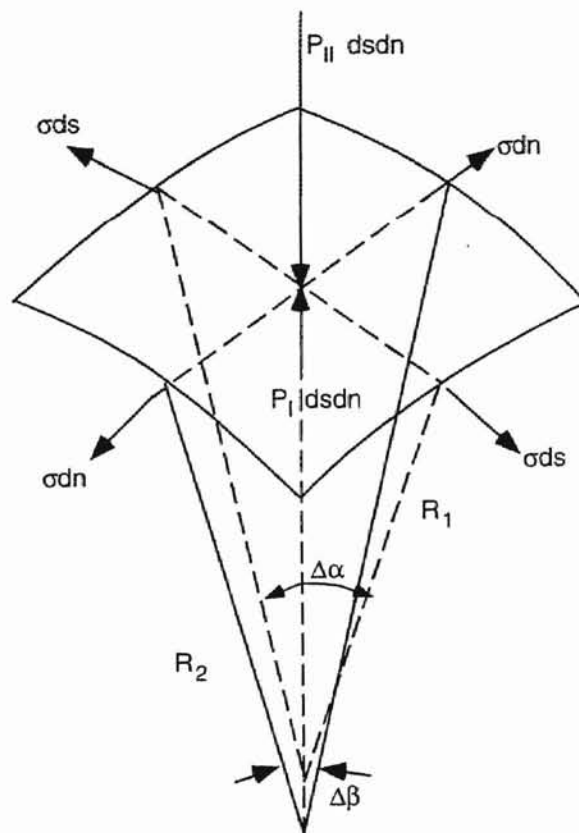


Figure 15: Force balance on a curved interface in 3 dimensions.

Since for the experimental setup, the web is assumed to be only curved in one direction, the equations above can be simplified according to Figure 16.

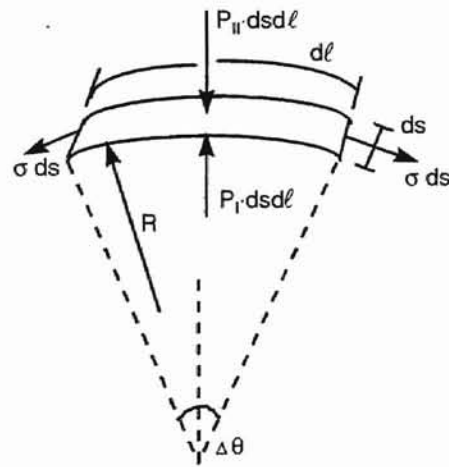


Figure 16: Two dimensional case

Now, the significant dimensions being ds , dl and the normal force as before called σ , the pressure difference across the curved surface can be written as follows.

Note, that the web is curved in only one direction now. Therefore the normal force can now be replaced by the tension. (σ now describing the tension in the web.)

Force Balance

$$(P_I - P_{II}) ds d\ell = 2\sigma ds \left(\sin \frac{\Delta\theta}{2}\right)$$

$$P_I - P_{II} = \frac{2\sigma}{d\ell} \cdot \frac{\Delta\theta}{2} = \frac{\sigma \cdot \Delta\theta}{d\ell}$$

with:

$$d\ell = \Delta\theta \cdot R$$

$$\Rightarrow P_I - P_{II} = \sigma \cdot \frac{1}{R} \quad \text{Eq. 2}$$

All these equations are derived from an infinite small section, that was taken out of the complete surface. The angles are assumed to be small, so the simplification

$$\sin\theta = \theta \quad \text{Eq. 3}$$

can be made.

The relationship derived gives the local pressure difference (ΔP) across the web in terms of the local tension (σ) in the web and its local radius of curvature (R).

$$\Delta P = \frac{\sigma}{R} \quad \text{Eq. 4}$$

ΔP : local pressure difference

σ : tension in the web

R : Radius of curvature

Since the local tension in the web can be measured, there is only one more parameter that needs to be determined and the local pressure or pressure difference can be calculated. This parameter is the radius of curvature. As mentioned earlier, the shape of the web needs to be known, because the radius of curvature can be calculated from the curvature, or the second derivative of the location itself.

The relationship between second derivative of location and radius of curvature can be written as

$$\frac{1}{R} = \frac{\frac{d^2 y}{dx^2}}{\sqrt{\left[1 + \left(\frac{dy}{dx}\right)^2\right]^{3/2}}}. \quad \text{Eq. 5}$$

Using this relationship, the local pressure difference can be expressed in terms of local web tension and local curvature, or second derivative of location. (Eq. 6)

$$\Delta P = \sigma \cdot \frac{d^2 y / dx^2}{\sqrt{\left[1 + \left(\frac{dy}{dx}\right)^2\right]^{3/2}}} \quad \text{Eq. 6}$$

With the information obtained about the web location, the second derivative can be found, and, together with the local tension, the pressure underneath the web at any given location (x-coordinate) can be determined.

As mentioned in chapter 2, the setup of the camera is at an angle. It was explained earlier, that this does not change the overall answers expected. The major forces and the significant motion are in the vertical plane. Taking a photograph from an angle of 15° from the horizontal makes it necessary to include the cosine of this angle into the calculations, but does not change the overall outcome of the observations. Any motion into the cross machine direction could be picked up with this camera. It is known that motion in the cross machine direction only arises from the forces in the vertical direction and a possible tilt angle. Thus assuring that the static curved web is not tilted will eliminate this problem. In case that any forces in the plane of the web are occurring, and they could change the position of the web in its plane, this motion would be reflected in the image of the web. But, since the angle of observation is small, any motion detected would go into the calculations with the sin of that angle. Because the motion itself is already small compared to any disturbances occurring in the vertical direction, this number would be insignificantly small and can therefore be neglected. For the calculations of the radius of curvature or the curvature itself, the following figure 17 explains how the cosine of the angle is important to the calculations.

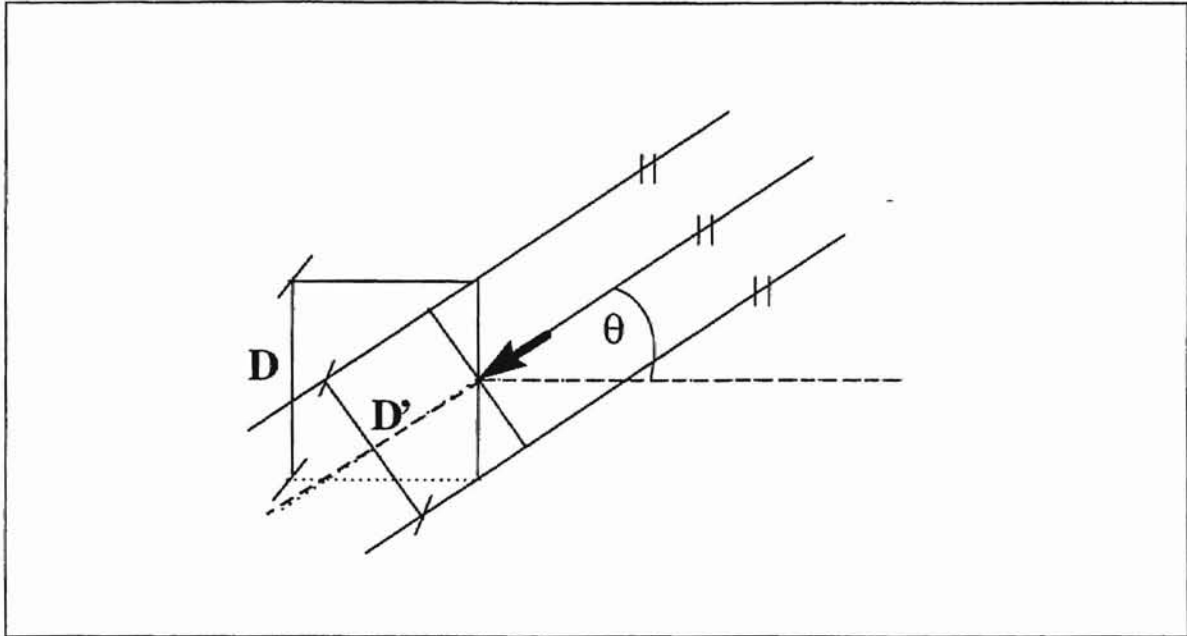


Figure 17: Distortion angle (θ) due to the angle under which the photograph is taken.

The projected height of the web, with respect to the support or any other reference point on the image, can be found as D' .

But, since the projected height is only the cosine fraction of the actual flotation height D of the web, the following relationship is valid.

$$D' = D \cdot \cos \theta \quad \text{Eq. 7}$$

Rearranging

$$D = \frac{D'}{\cos \theta} \quad \text{Eq. 8}$$

Applying the above derived equations and theories to the values obtained from the image analysis, gives the first and second derivative of the location of the web. Since the obtained coordinates are discrete values, the derivatives have to be approximated. In this case, the finite difference method was used.

To keep the information as locally concentrated as possible, which means not to average over a wide range of points, the 3-point formula was used to approximate the first and second derivative for the data for the pixel locations, gained earlier.

For the first derivative this can be written as in Eq. 9

$$\left. \frac{df}{dx} \right|_{x=x_i} = \frac{1}{2} \cdot (-f(x_i - 1) + f(x_i + 1)) \quad \text{Eq. 9}$$

The left hand(x_0) - and right hand(x_N) borders are approximated by the equations Eq. 10 and Eq. 11.

$$\left. \frac{df}{dx} \right|_{x=x_0} = \frac{1}{2} \cdot (-3 \cdot f(x_0) + 4 \cdot f(x_1) - 1 \cdot f(x_2)) \quad \text{Eq. 10}$$

$$\left. \frac{df}{dx} \right|_{x=x_N} = \frac{1}{2} (1 \cdot f(x_{N-2}) - 4 \cdot f(x_{N-1}) + 3 \cdot f(x_N)) \quad \text{Eq. 11}$$

The finite difference method gives the following expressions for the second derivative, or the curvature, if using the 3-point central differencing.

$$\left. \frac{d^2 f}{dx^2} \right|_{x=x_i} = \frac{2}{2} \cdot (1 \cdot f(x_{i-1}) - 2 \cdot f(x_i) + 1 \cdot f(x_{i+1})) \quad \text{Eq. 12}$$

The left - and right hand side (x_0 and x_N) follow the same equation..

$$\left. \frac{d^2 f}{dx^2} \right|_{x=x_0} = \frac{2}{2} (1 \cdot f(x_0) - 2 \cdot f(x_1) + 1 \cdot f(x_2)) \quad \text{Eq. 13}$$

$$\left. \frac{d^2 f}{dx^2} \right|_{x=x_N} = \frac{2}{2} (1 \cdot f(x_{N-2}) - 2 \cdot f(x_{N-1}) + 1 \cdot f(x_N)) \quad \text{Eq. 14}$$

When the results were plotted over the horizontal axis, it was seen that the first as well as second derivative included large errors. (displayed in blue in Figs. 18 and 19)

The curves showed jumps from negative to positive values, which decreased the actual amount of valuable local information that was obtained. To reduce the error, apparently produced by the finite differences, the five point formula for the first and second

derivative was used. This gave an average over five neighboring points, while weighing the actual point of interest higher than the neighbor values. (Eq. 15 - 24)

$$\left. \frac{df}{dx} \right|_{x=x_i} = \frac{1}{24} \cdot (2 \cdot f(x_{i-2}) - 16 \cdot f(x_{i-1}) + 16 \cdot f(x_{i+1}) - 2 \cdot f(x_{i+2})) \quad \text{Eq. 15}$$

$$\left. \frac{d^2f}{dx^2} \right|_{x=x_i} = \frac{2}{24} \cdot (-1 \cdot f(x_{i-2}) + 16 \cdot f(x_{i-1}) - 30 \cdot f(x_i) + 16 \cdot f(x_{i+1}) - 1 \cdot f(x_{i+2})) \quad \text{Eq. 16}$$

for: $2 \leq i \leq N - 2$

For the first derivative, the finite difference equations, as the left hand side of the image is approached, are given in the following expressions (Eq. 17 and 18)

$$\left. \frac{df}{dx} \right|_{x=x_0} = \frac{1}{24} \cdot (-50 \cdot f(x_0) - 96 \cdot f(x_1) - 72 \cdot f(x_2) + 32 \cdot f(x_3) - 6 \cdot f(x_4)) \quad \text{Eq. 17}$$

$$\left. \frac{df}{dx} \right|_{x=x_1} = \frac{1}{24} \cdot (-6 \cdot f(x_0) - 20 \cdot f(x_1) + 36 \cdot f(x_2) - 12 \cdot f(x_3) + 2 \cdot f(x_4)) \quad \text{Eq. 18}$$

and for the second derivative, they can be written as in Eqs. 19 and 20.

$$\left. \frac{d^2f}{dx^2} \right|_{x=x_0} = \frac{2}{24} \cdot (35 \cdot f(x_0) - 104 \cdot f(x_1) + 114 \cdot f(x_2) - 56 \cdot f(x_3) + 11 \cdot f(x_4)) \quad \text{Eq. 19}$$

$$\left. \frac{d^2f}{dx^2} \right|_{x=x_1} = \frac{2}{24} \cdot (11 \cdot f(x_0) - 20 \cdot f(x_1) + 6 \cdot f(x_2) + 4 \cdot f(x_3) - 1 \cdot f(x_4)) \quad \text{Eq. 20}$$

If the right hand border of the field of data is approached the Eq. 21 and Eq. 22 can be used to calculate the first derivative for the two endpoints.

$$\left. \frac{df}{dx} \right|_{x=x_N} = \frac{1}{24} \cdot (-2 \cdot f(x_{N-4}) + 12 \cdot f(x_{N-3}) - 36 \cdot f(x_{N-2}) - 20 \cdot f(x_{N-1}) + 6 \cdot f(x_N))$$

Eq. 21

$$\left. \frac{df}{dx} \right|_{x=x_{N-1}} = \frac{1}{24} \cdot (6 \cdot f(x_{N-4}) - 32 \cdot f(x_{N-3}) + 72 \cdot f(x_{N-2}) - 96 \cdot f(x_{N-1}) + 50 \cdot f(x_N))$$

Eq. 22

Similarly the second derivative is expressed through Eqs. 23 and 24.

$$\left. \frac{d^2f}{dx^2} \right|_{x=x_N} = \frac{2}{24} \cdot (-1 \cdot f(x_{N-4}) + 4 \cdot f(x_{N-3}) - 6 \cdot f(x_{N-2}) - 20 \cdot f(x_{N-1}) + 11 \cdot f(x_N))$$

Eq. 23

$$\left. \frac{d^2f}{dx^2} \right|_{x=x_{N-1}} = \frac{2}{24} \cdot (11 \cdot f(x_{N-4}) - 56 \cdot f(x_{N-3}) + 114 \cdot f(x_{N-2}) - 104 \cdot f(x_{N-1}) + 35 \cdot f(x_N))$$

Eq. 24

Both averaging methods (over 3 and over 5 points) are displayed in the following diagrams. Fig. 18 shows the central difference approximation for the first derivative of the detected location, Fig. 19 shows the approximation for the second derivative, or curvature.

The central difference over 3 neighboring values is shown as blue line, whereas the one using five values is shown in pink.

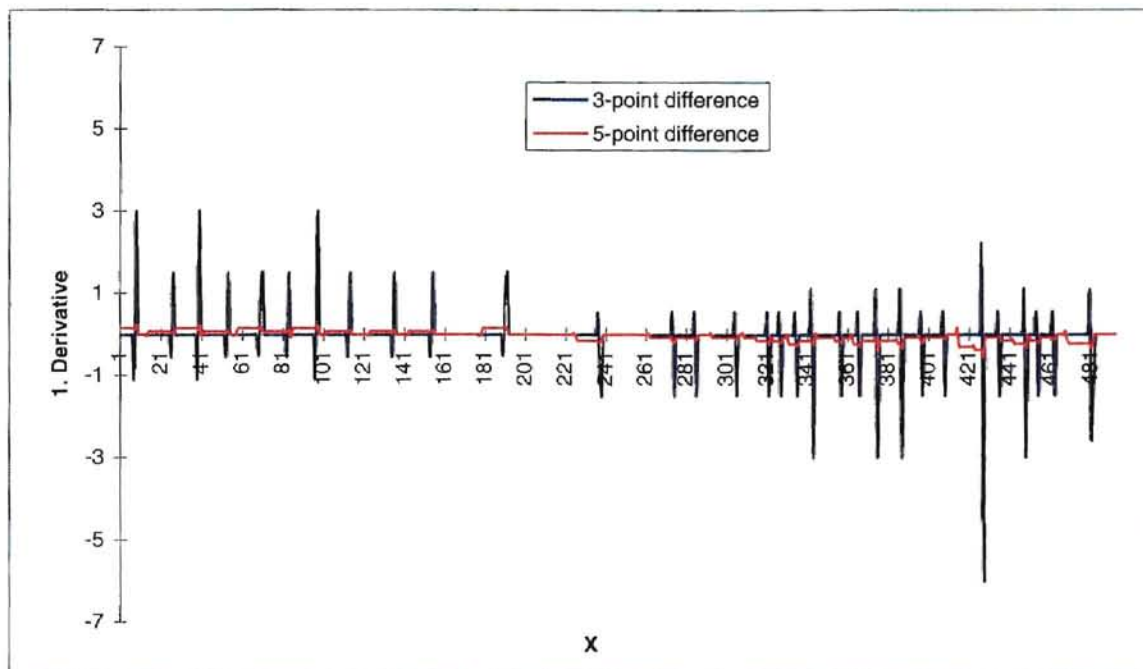


Figure 18: First derivative, approximated by central differences for the location y over x.

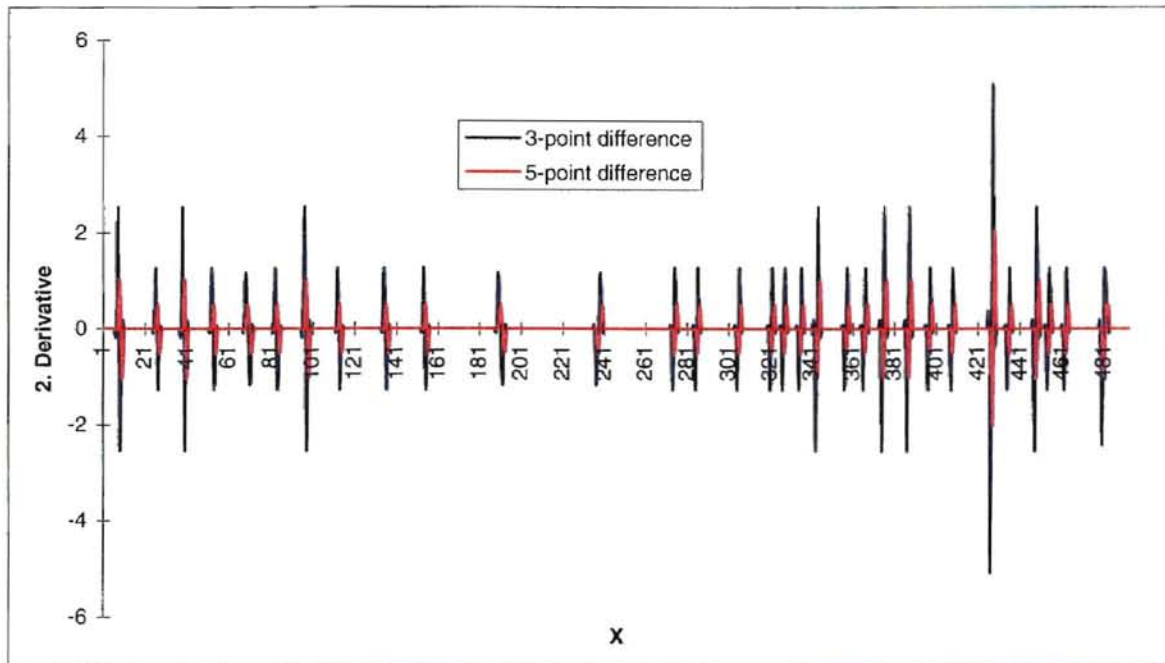


Figure 19: Second derivative as approximated by the central differences, for the location y over x .

6. OBSERVATIONS

As can be seen in figs. 18 and 19, the outcome is not as good as expected. Even though, the five-point formula gives smoother results for the first derivative, it still does not reduce the errors in the second derivative. Unfortunately, the second derivative is of far more importance than the first derivative. The second derivative needs to be used to calculate the radius of curvature, according to the equations derived in the earlier chapter. With this information the final result should be able to predict the local pressure underneath the web.

This means that the occurring errors in the second derivative are fatal for the locally needed information. For the calculations of the overall forces, this is not as critical and therefore does not need to be discussed. Overall forces are the integral of local forces along a surface. Therefore, any local information is being erased. This phenomenon is only critical in connection with the locally needed information.

The reason that these errors occur is because the shape of the web is being represented by points or pixels, when capturing the photograph with the framegrabber board. Digitizing the image leaves only one or two significant digits. Only a complete pixel can be stored

as being part of the center line, not a part of the pixel. This means that the actual continuous line is being discretized and therefore a lot of local information lost at this point. Another reason that these errors seem so crucial is that the vertical range of pixels is only 10 to 20, at the most. This means that the center line, that is of interest in this project spreads in the horizontal direction over the full 496 pixel points, whereas its vertical range is only 20 pixel points out of 372 possible points. The less curved the web is, the less is its vertical range in terms of pixel representation. Because only 3% to 6% of the actual possible points are used to describe the location of the black centerline, the errors showing in the second derivative are actually located not in the finite difference method, but in the way the image is stored in the computer.

The original approach using only a 3-point central difference method will amplify these errors. This means that there is a trade-off between local information that is needed, and averaging techniques that need to be applied to obtain reasonable results. The following chapter discusses solutions to this problem.

7. DISCUSSION

7.1. Influence of the Resolution

Because the main problem arises whenever the image is digitized, that process should be modified. Once the image is stored, only one significant digit is left. This cannot be changed. What can be changed is the resolution of the image, by either using a high resolution camera, or a frame grabber that can capture more pixels in both directions, or both.

The disadvantage with this solution is, that a high resolution camera is very expensive and does not give the optimum output. These cameras as well as a frame grabber board with higher resolution digitize more pixels in both directions. This is not really the desired effect.

7.2. Vertical Distortion

More desirable would be to have a distortion effect only in the vertical direction. This would change the rate of pixels used in the vertical direction with respect to the ones used

in the horizontal direction. A cylindrical lens is one possible device for this. There are computer techniques to distort images in one or another direction, but this is not a possible solution, because in order to manipulate the image with an image processing software package, the picture needs to be already digitized. This means that valuable local information is already lost. Anything done to it at this point is not going to recover the original image, and with it the local information that was lost. Any kind of distorting of the photograph has to be done prior to digitizing and, therefore, photo optical techniques need to be applied, like the cylindrical lens.

This optical technique can be simulated on the computer. In order to examine whether the vertical distortion is an acceptable method to improve the data analysis, the basic principle was simulated by generating a polynomial function of second degree (of type $f(x)=a \cdot x^2+c$). The graph of the function was plotted, and with the help of a video camera, and a framegrabber board, digitized and stored in the PC. The procedure used is exactly the same as used before with the photographs from the laboratory setup. The pixel intensities were analyzed, as described in earlier chapters. The result of the data analysis is shown in Fig. 20 and 21. Notice that the curve now stretches over a wide range of vertical pixels as well as horizontal pixels. As can be seen from the figures below, the shape of the web does not influence the results in the second derivative as expected. Obviously a wider range in the vertical direction is not the solution to the discretization problem. As can be seen in Fig. 21 there are still enormous local errors, which cannot be

tolerated for the further analysis of the data. The resolution seems to be a more critical problem in this application than originally stated.

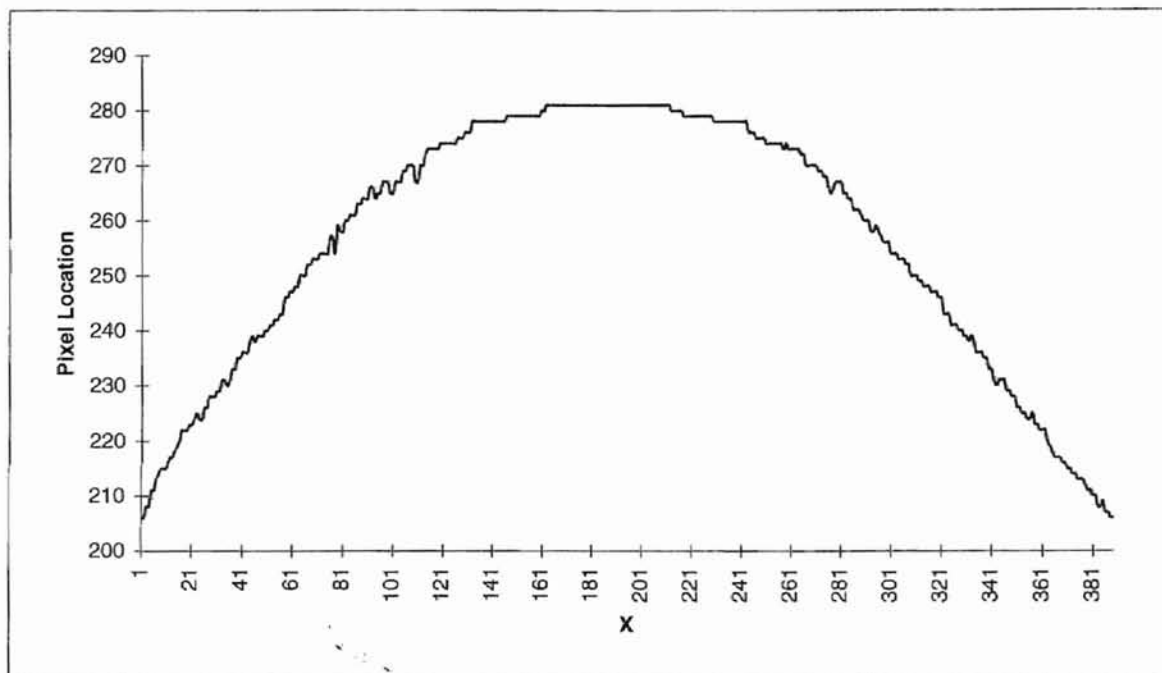


Figure 20: Polynomial function as detected and stored in the PC.

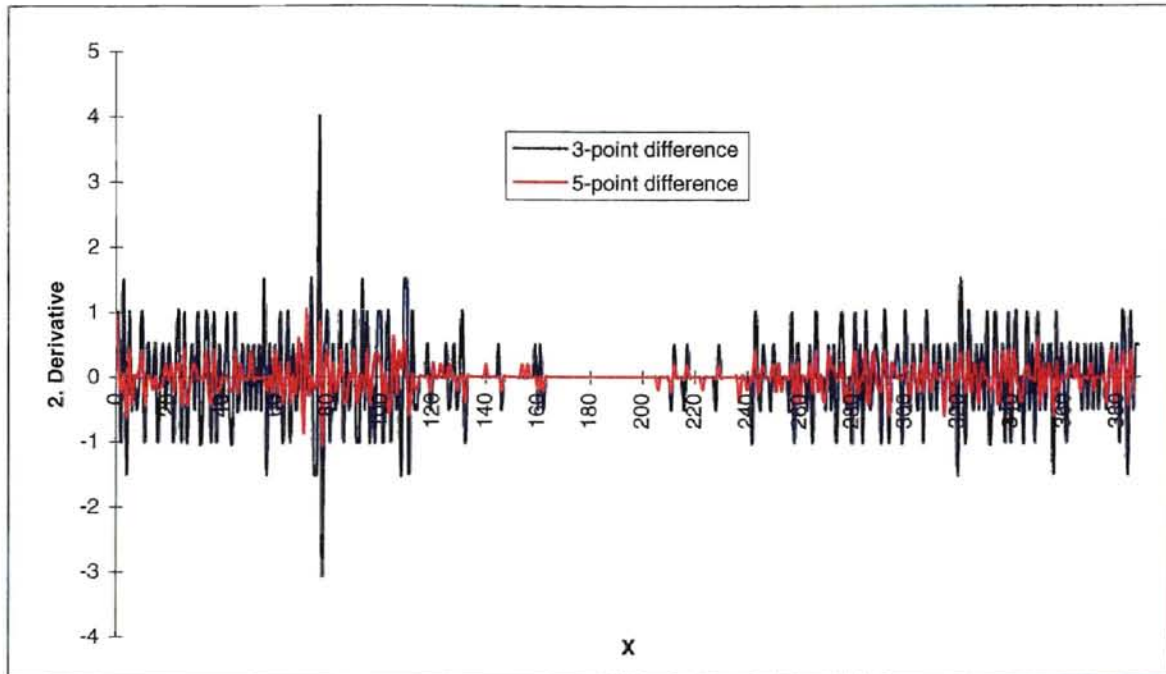


Figure 21: Second derivative as approximated by the central differences, for the location y over x . (Again the blue shows the 3-point formula, and the pink the 5-point formula.)

7.3. Overlay Several Images

The analysis of a sequence of images may be another solution. Although averaging over a sequence of pictures will reduce the noise picked up, it is very questionable if noise reduction really will reduce the error brought into the image by digitizing it.

7.4. Curve Fit

A fourth method, that could be applied, is a curve fit. The points obtained by the software program are discrete values. A curve fit along through the points of vertical displacement, gives the advantage, that the first and second derivative can be directly taken from a function, that will describe the relationship between the x- and y- coordinates. Also, curve fitting will actually gain back lost information. Because the most important information, that the web is a continuous material is being lost by giving each x-location one exact y-location with no possible decimal point, the curve fit does take advantage of this information about the continuity and therefore will be able to regain information that was lost with the discretization of the photograph. This method was applied to the computer generated plot as well as to the picture taken in the laboratory of the experimental setup.

The following figures (Fig. 22 and 23) show the result if the detected curve is modeled with a sin-wave (pink line) or a polynomial function (yellow line). Fig. 22 is the simulated web curve which ranges over $\frac{1}{2}$ of the possible vertical pixel locations. Fig. 23 is the original lab photography, after being scanned into the computer and analyzed by the created software.

Obviously the polynomial function described the simulated curve better, because it was originally created through a second degree polynomial function. The sin-function is as

well a good approximation and as can be seen in Fig. 24, both can interchangeably be used for the original image.

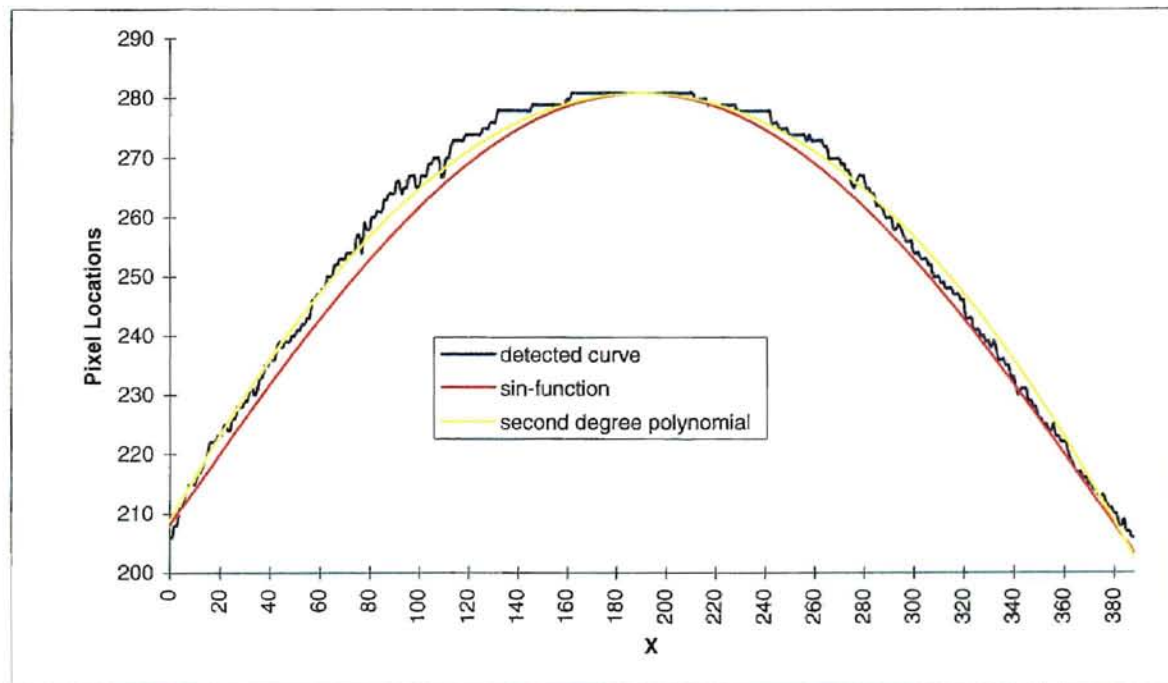


Figure 22: Simulated curve as it is digitized by the frame grabber (blue) and its curve fit (sin-function = pink, polynomial = yellow).

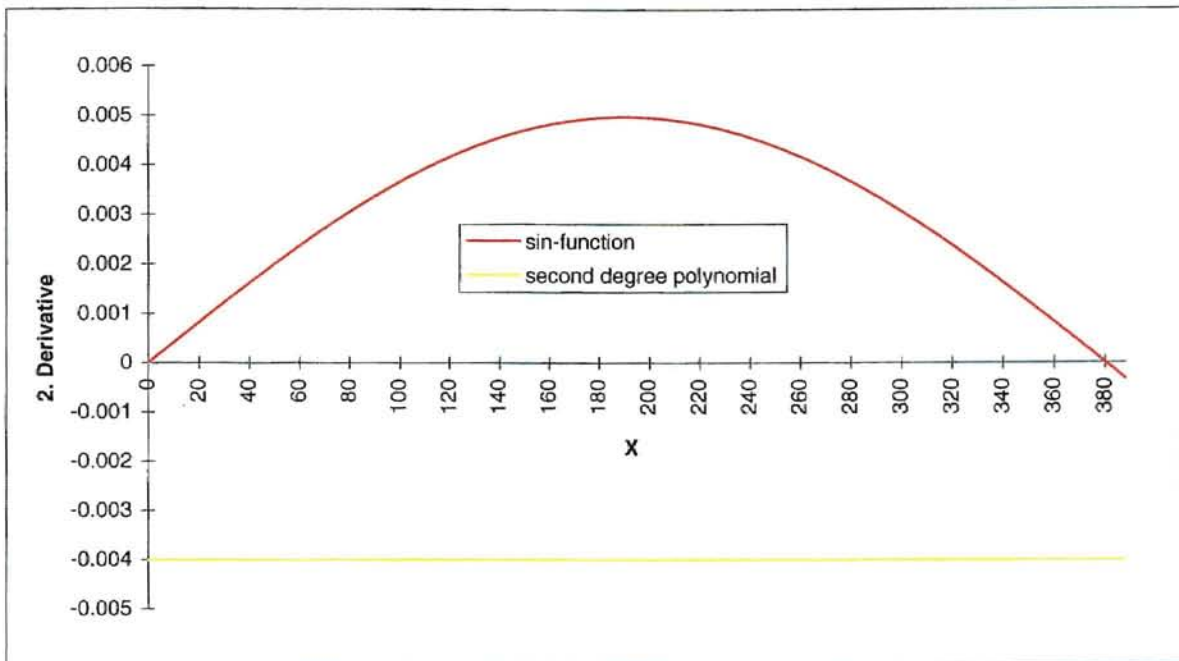


Figure 23: Second derivative using the derivative of the curve fit

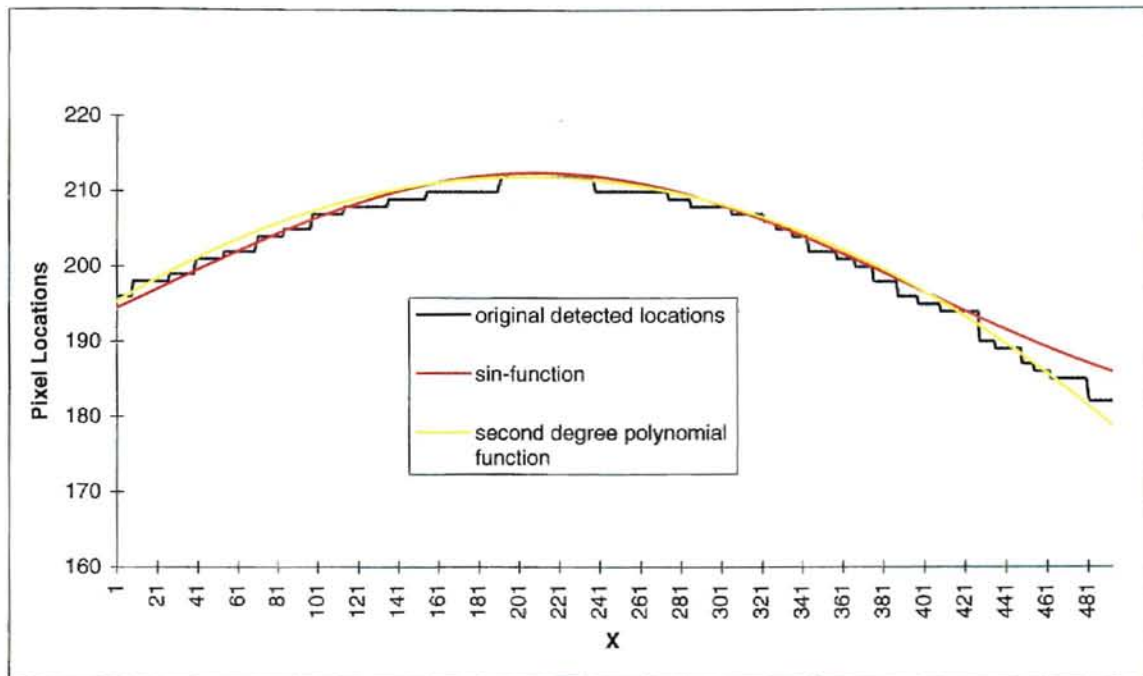


Figure 24: Curve detected from the original photograph and the curve fit with a sin-function (pink) and a second degree polynomial (yellow).

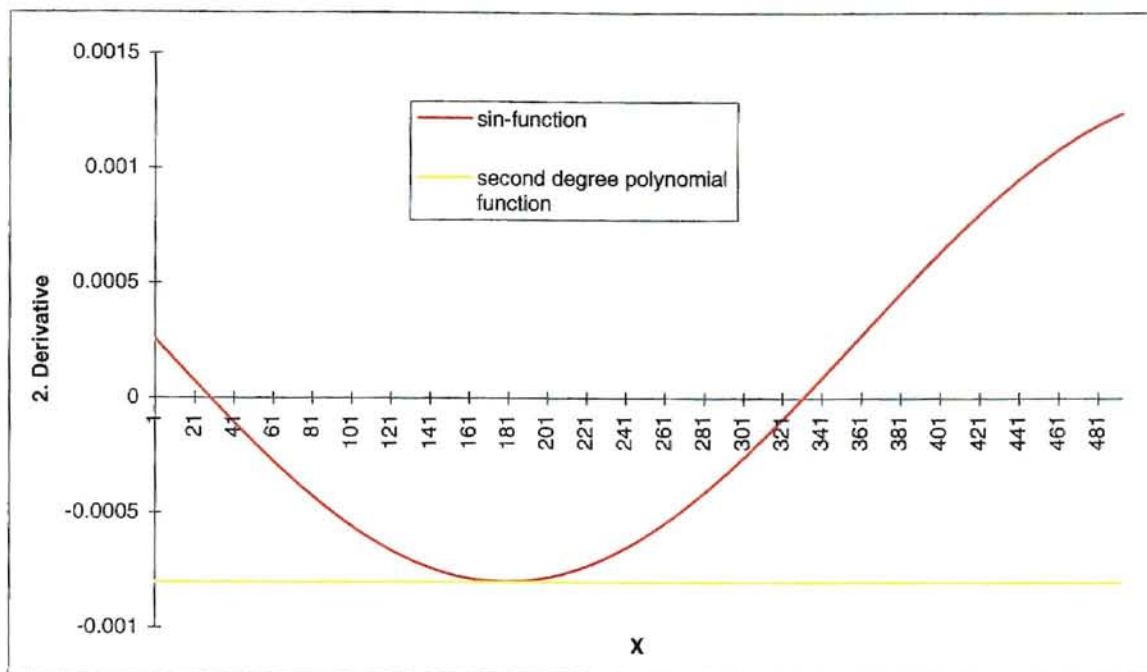


Figure 25: Second derivative applied to the curve fit of the original laboratory setup. (pink = derivative of the sin-function, yellow = derivative of the polynomial).

The question whether the sin-function or a second degree polynomial function describe the original curve better needs some further analysis. Depending on the particular case being looked at one or the other will be a better fit. Pressure measurements and comparison with the calculated data from the curve fit will also help to determine, whether both functions can be used interchangeably for all cases. Looking at a web line and the shape the web is taking while being transported through the flotation oven, suggests that the sin-function will be a better approximation on a web line.

8. CONCLUSIONS

The principal idea in this project was to show that without any specialized equipment, using only a video camera, a frame grabber and an IBM compatible PC, the contour of a web can be detected and analyzed, in order to determine shape, changes in shape and the forces acting on a web transported over an air bar.

Real time analysis of the web and its motion is, with this equipment, not possible, because the analysis is too time intensive. One frame takes more than two seconds to analyze and store the data. Also, the frame grabber is not capable of capturing 30 or more frames per second.

Still, the dynamic behavior of the web can be analyzed by simply comparing the images that are recorded with the video camera. Comparing these sequences frame by frame gives information about the dynamic motion of the web. This method cannot be used to interact with a controller and used as feedback to regulate the web position, but it can certainly give valuable information about the change in position.

Digitizing and then numerically comparing the shape has the disadvantage that too much detail gets lost. The one or two significant digits that will describe the position of the web are only an approximation, which mathematically changes the results expected.

9. FUTURE WORK

The future work in this project should be to look at different possibilities to enhance the numerical results. As mentioned before, this could be a high resolution camera, or/and applying a curve fit to the values obtained from the software. As shown in chapter 6, the vertical distortion is not the ultimate answer to the problem. A camera and/or frame grabber, which are able to digitize more pixel per inch, would certainly be an improvement.

More expensive and sophisticated hardware is not necessarily the right and only answer to the problems discovered here, but a frame grabber, that can capture and store a sequence of images per second, is one step advancing towards the real time application.

The curve fitting, as described in chapter 6, certainly increases the information, and gains lost detail back, because it makes use of the continuity of the web. This can be applied to either already existing images or new pictures, whether a high resolution video camera and frame grabber are used or not.

CITED WORK

[1] Acton, Dr. S.

“Digital Image Processing”, Lecture Notes for ECEN 5793

Oklahoma State University, 1994

[2] Moretti, Dr. P.M.

“Coupling between Out-of-Plane Displacement and Lateral Stability of Webs in Air-Support Ovens”,

Oklahoma State University, Oct. 1993

[3] Nisankararao, S. K.-V.

“An Experimental Study of Aerodynamic Forces of Air Bars”,

M.S. Thesis, Oklahoma State University, 1994

[4] Perdue, D.

“Lateral Stability Investigation of Air Bar and Web Interaction for Use in Flotation Ovens”,

M.S. Thesis, Oklahoma State University, 1993

[5] Pinnamaraju, R.

“Measurements on Air Bar/Web Interaction for the Determination of Lateral Stability of a Web in Flotation Ovens”,

M.S. Report, Oklahoma State University, 1992

VITA ²

Brigitte Busch

Candidate for the Degree of

Master of Science

Thesis: MEASUREMENTS ON AIR BAR/WEB INTERACTION FOR THE
DETERMINATION OF STABILITY OF A WEB

Major Field: Mechanical Engineering

Biographical:

Personal Data: Born in Cologne, Germany, March 25, 1968, the daughter of Mr. Manfred Busch and Mrs. Ursula Busch.

Education: Graduated from Gymnasium Nieder-Olm, Nieder-Olm, Germany, June, 1987; received a Degree in Mechanical and Aerospace Engineering (Diplom-Ing.) from Technische Universitaet Muenchen, Munich, Germany, Oct. 1993; completed requirements for the Master of Science Degree at Oklahoma State University, July, 1997.

Professional Experience: Internship at BMW, Munich Germany, in the summer of 1991; employed as a research engineer, by Euraplan, Munich, Germany in 1993; employed as a graduate research and graduate teaching assistant and Lecturer, Oklahoma State University of General Engineering, Oklahoma State University, Department of Mechanical and Aerospace Engineering, 1993 to present.

Professional Organizations: Royal Aeronautical Society, Munich Branch (RAe); American Institute of Aeronautics and Astronautics (AIAA).

Honors and Awards: Phi Kappa Phi Member, 1996